Recognition of apoptotic cells by viable cells is specific, ubiquitous, and species independent: analysis using photonic crystal biosensors

Goutham Pattabiraman[a], Erich A. Lidstone[b], Karol Palasiewicz[a], Brian T. Cunningham[b,c,d], and David S. Ucker[a,d,e]

[a]Department of Microbiology and Immunology, [d]Cancer Center, and [e]Department of Bioengineering, University of Illinois College of Medicine, Chicago, IL 60612; [b]Department of Bioengineering and [c]Department of Electrical and Computer Engineering, University of Illinois at Urbana–Champaign, Urbana, IL 61801

ABSTRACT **Apoptotic recognition is innate and linked to a profound immune regulation (innate apoptotic immunity [IAI]) involving anti-inflammatory and immunosuppressive responses. Many of the molecular and mechanistic details of this response remain elusive. Although immune outcomes can be quantified readily, the initial specific recognition events have been difficult to assess. We developed a sensitive, real-time method to detect the recognition of apoptotic cells by viable adherent responder cells, using a photonic crystal biosensor approach. The method relies on characteristic spectral shifts resulting from the specific recognition and dose-dependent interaction of adherent responder cells with nonadherent apoptotic targets. Of note, the biosensor provides a readout of early recognition-specific events in responder cells that occur distal to the biosensor surface. We find that innate apoptotic cell recognition occurs in a strikingly species-independent manner, consistent with our previous work and inferences drawn from indirect assays. Our studies indicate obligate cytoskeletal involvement, although apoptotic cell phagocytosis is not involved. Because it is a direct, objective, and quantitative readout of recognition exclusively, this biosensor approach affords a methodology with which to dissect the early recognition events associated with IAI and immunosuppression.**

Monitoring Editor
Carl-Henrik Heldin
Ludwig Institute for Cancer Research

Received: Dec 2, 2013
Revised: Mar 11, 2014
Accepted: Mar 26, 2014

INTRODUCTION

The interaction of apoptotic cells (referred to here as "targets") with viable cells ("responders") elicits a variety of outcomes in the responding cells, most comprehensively characterized as anti-inflammatory (Meagher *et al.*, 1992; Voll *et al.*, 1997; Fadok *et al.*, 1998a; Cocco and Ucker, 2001; Savill *et al.*, 2002; Ren *et al.*, 2008). We and others have shown that apoptotic cells affect the proinflammatory transcriptional machinery of macrophages and other responder cells with which they interact, independent of Toll-like receptor signaling (Cvetanovic and Ucker, 2004; Kim *et al.*, 2004; Chung *et al.*, 2007; Xiao *et al.*, 2008). Recognition and inflammatory modulation represent key elements of an innate immune response (innate apoptotic immunity [IAI]) that discriminates live from effete cells (Birge and Ucker, 2008).

The ability of apoptotic cells to be recognized and modulate proinflammatory responses represents paradoxically a gain of function acquired during the physiological cell death process. The immunomodulatory activity of apoptotic targets is manifest as immediate-early effects on transcription in responder cells (Cvetanovic and Ucker, 2004). These effects depend generally on direct responder cell contact with the apoptotic targets (i.e., they are abrogated when targets and responders are physically separated by otherwise permeable barriers) but are independent of target cell phagocytosis. For example, pharmacologic interference with cytoskeletal (actin or tubulin) polymerization (with cytochalasin D or

This article was published online ahead of print in MBoC in Press (http://www.molbiolcell.org/cgi/doi/10.1091/mbc.E13-11-0700) on April 2, 2014.

Address correspondence to: David Ucker (duck@uic.edu), Brian Cunningham (bcunning@illinois.edu).

Abbreviations used: CFDA, 5(6)-carboxyfluorescein diacetate succinimidyl ester; IAI, innate apoptotic immunity; PWV, peak wavelength value; SUPER, surface exposed during apoptotic cell death, ubiquitously expressed, protease-sensitive, evolutionarily conserved, and resident normally in viable cells.

colchicine, respectively) prevents target cell engulfment but has no effect on the responses, including immune modulation, elicited by those apoptotic targets (Reddy *et al.*, 2002; Cvetanovic and Ucker, 2004). Although molecules involved in the engulfment of apoptotic cells (including phosphatidylserine and its various receptors) have been studied extensively, the molecules involved in the initial events of recognition and triggering of immune modulation remain undefined (Devitt *et al.*, 1998; Fadok *et al.*, 1998b; Schlegel and Williamson, 2001; Scott *et al.*, 2001; Hanayama *et al.*, 2002; Arur *et al.*, 2003; Miyanishi *et al.*, 2007; Gude *et al.*, 2008; Elliott *et al.*, 2009).

The recognition-dependent interactions leading to the binding of targets by responders can be visualized microscopically, but a convenient assay for binding per se is lacking. Previously we were able to quantify binding using an objective fluorescence-based microwell assay that monitors the extent to which fluorescently labeled (nonadherent) target cells become associated with (adherent) responder cells (Cocco and Ucker, 2001). That approach depends on the continued adhesion of responders and the ability to remove unbound targets by washing. This is a significant technical limitation, and the assay is defeated in cases in which target cells and washing disrupt responder cell adhesion. More recent studies avoided direct assessment of recognition and relied instead on more convenient and sensitive measurements that use anti-inflammatory readouts. For example, because the ability of apoptotic cells to modulate inflammatory responses occurs primarily on the level of transcription, transcriptional reporters that disclose primary inflammatory responses (i.e., transcriptional promoters linked to the firefly luciferase gene and responsive to critical transcriptional activators involved in inflammatory responses, such as NFκB) serve as convenient and reliable readouts of apoptotic recognition (Cvetanovic and Ucker, 2004; Cvetanovic *et al.*, 2006). Other early responses to apoptotic targets, including the distinct effects they exert upon the activation of families of mitogen-activated protein kinases in responder cells, also provide characteristic indicators (Cvetanovic *et al.*, 2006; Patel *et al.*, 2006, 2007). These indirect measures, however, cannot probe the proximal events of recognition.

We endeavored to develop a technically simple and direct approach by which to quantify apoptotic recognition. We observed that apoptotic cell binding is associated with slight alterations in responder cell morphology (especially spreading). Because biosensors have been used successfully to assess adhesion, we imagined that the biosensors also could be used in this case. This use of biosensors in this context, in fact, has been successful and has provided a direct readout of target cell binding.

The photonic crystal biosensors used in this work are one-dimensional periodic grating surface structures (period, 550 nm) formed with a low–refractive index polymer on a transparent polyester sheet coated with a high–refractive index TiO_2 film and comprising the bottoms of 96-well-format microplates (Cunningham *et al.*, 2004). The sensors are a periodic arrangement of dielectric materials, the geometry of which generates an electromagnetic standing wave. This electromagnetic field, generally referred to as an "evanescent electromagnetic field," is confined to an ~200-nm region in the medium above the photonic crystal surface and exhibits exponentially decaying field magnitude. The photonic crystal surface is a narrowband wavelength reflectance filter by which the sensor reflects light at the resonant wavelength with nearly 100% reflection efficiency while allowing all other wavelengths to be transmitted through the sensor structure. The sensor operates by manifesting changes in the wavelength of reflected light as molecular or cellular events take place within the evanescent field region adjacent to the biosensor surface. The resonant reflected wavelength of the sensor (peak wavelength value [PWV]) can be measured by illuminating the photonic crystal at normal incidence with white light and measuring the reflected light spectrophotometrically. Cell-associated changes in the PWV of reflected light (ΔPWV) are consequences of incompletely defined cellular events (Chan *et al.*, 2007), which have been referred to alternatively as intimate biosensor contacts, the density of attachment within the detection zone, proximal relocation of cellular contents toward the biosensor surface, and increased dielectric permittivity or increased mass associated with the biosensor surface (Shamah and Cunningham, 2011). This is somewhat analogous to the detection of resonance oscillations (surface plasmon resonance) triggered by photon excitation of planar metallic surfaces to which proteins or other pure molecular species are adhered, which are subject to alterations as a function of molecular interactions, such as ligand binding (Guo, 2012).

We observed discrete spectral shifts (ΔPWV) reflective of the binding by adherent viable responder cells of apoptotic target cells occurring distal to the biosensor surface and distinct from responder cell adhesion-specific ΔPWV. Here we describe this novel methodology for examining cellular recognition and some resulting findings.

RESULTS

The interaction of adherent responder cells with apoptotic target cells is discernible with the photonic crystal biosensor

We demonstrated previously that the ability of viable cells to recognize and respond to apoptotic targets reflects a specific and innate process present ubiquitously in professional and nonprofessional phagocytes and nonphagocytic cell types alike. Apoptotic determinants for recognition and immune modulation are protease sensitive and evolutionarily conserved molecules that arise on the surface of cells during the process of apoptotic death, without a requirement for ensuing new gene expression. We used the acronym SUPER (surface exposed during apoptotic cell death, ubiquitously expressed, protease-sensitive, evolutionarily conserved, and resident normally in viable cells) to capture these defining properties of apoptotic recognition determinants (Ucker *et al.*, 2012). Our conclusions regarding recognition are derived from direct measurements of apoptotic cell binding, using a fluorescence-based microwell binding assay (Cocco and Ucker, 2001) and, by inference, measuring responses to apoptotic cells dependent upon their recognition (Cvetanovic and Ucker, 2004).

The ability of apoptotic cells ("targets") to modulate inflammatory responses in viable responder cells ("responders") occurs primarily on the level of transcription and can be assessed reliably with transcriptional reporters that disclose primary inflammatory responses (i.e., transcriptional promoters linked to the firefly luciferase gene and responsive to critical transcriptional activators involved in inflammatory responses, such as NFκB; Cvetanovic and Ucker, 2004; Cvetanovic *et al.*, 2006). B2.1 is an example of a highly responsive clone of human HEK293T cells stably transfected with such an NFκB-dependent transcriptional reporter (Cvetanovic *et al.*, 2006). Although the robust and specific transcriptional response of B2.1 responder cells to apoptotic targets reflects target cell recognition, we did not previously assess apoptotic recognition per se in these cells.

We asked whether we could detect the initial binding-related events associated with the recognition of apoptotic cells, which precede transcriptional responses, in B2.1 responder cells, using photonic crystal biosensors. B2.1 cells were seeded into biosensor wells. Incubation of those cells in wells with a biosensor bottom surface

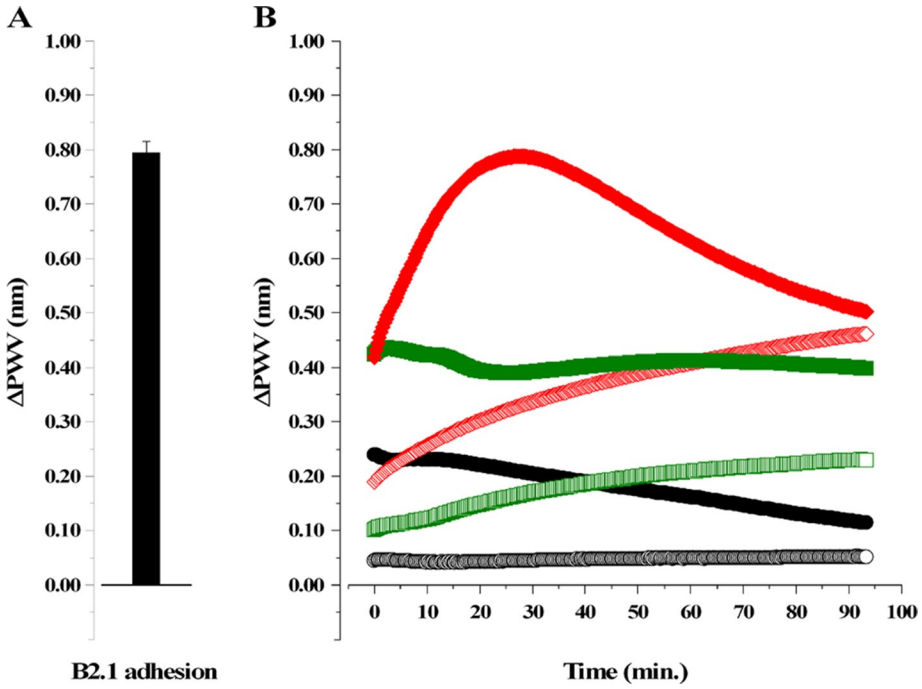

FIGURE 1: A characteristic resonant wavelength shift (ΔPWV), distinct from an adhesion-specific ΔPWV, results from the interaction of adherent responder cells with apoptotic target cells. (A) The change in peak (reflected light) wavelength value (ΔPWV) associated with adhesion ($\Delta PWV_{adhesion}$) of human B2.1 responder cells to the biosensor surface of microwells was determined. Responder cells were plated 12 h earlier at 1×10^5 cells/well and incubated overnight at 37°C. Data are presented as the mean (±SEM) of triplicate determinations. (B) The interaction of target cells (Jurkat cells, either viable or induced to die apoptotically with actinomycin D) with adherent B2.1 responder cells was monitored in biosensor microwells in which responder cells had been previously seeded. Targets (1×10^6 cells/well) were added to wells (target:responder ratio = 10:1). Data acquisition in the BIND reader (25°C) was begun immediately. The data presented are the means of triplicate single-well determinations. SEMs are less than ±0.05 nm in all cases; for clarity, SEMs are not shown. The experiment was repeated independently >10 times. Peak (reflected light) wavelength values (PWV) were determined initially for each well without cells (medium only, $PWV_{initial}$). Changes in PWV (ΔPWV) then were determined for each well after incubation overnight (o/n) with medium only (○, $\Delta PWV_{medium} = PWV_{medium\ o/n} - PWV_{initial}$) or B2.1 responder cells (●, $\Delta PWV_{adhesion} = PWV_{responder\ cells\ o/n} - PWV_{initial}$). Finally, kinetic measurements were acquired after the addition of apoptotic (◇) or viable (□) targets to wells incubated overnight with medium only or the addition of apoptotic (◆) or viable (■) targets to wells incubated overnight with B2.1 responders. Changes in PWV (ΔPWV) then were calculated as $\Delta PWV_{targets\ only} = PWV_{targets\ only} - PWV_{medium\ o/n}$ and $\Delta PWV_{interaction} = PWV_{targets\ +\ responder\ cells} - PWV_{responder\ cells\ o/n}$. (Tracings represent calculated ΔPWV determinations from real-time data acquisition; it is easiest to discern the symbol from the last time point of each tracing.) Differences of PWV values between wells with and without responder cells ($\Delta PWV_{adhesion}$) are significant ($p < 0.001$; Student's two-tailed paired *t* test). Differences of PWV values between wells with responder cells to which targets were added ($\Delta PWV_{interaction}$) or to which target cells were not added are highly significant ($p < 0.0001$; two-way ANOVA). Differences of PWV values between wells with responder cells to which apoptotic or viable targets were added also are highly significant ($p < 0.0001$; two-way ANOVA).

led to their adhesion (which was evident by microscopic visualization) and resulted in a corresponding shift in the peak wavelength value (ΔPWV) of reflected resonant light (Figure 1A). (Note that $\Delta PWV_{adhesion}$ is calculated for each well independently, with the initial observed value of an individual well [$PWV_{initial}$] subtracted from the measured postadhesion value of the same well.)

When apoptotic targets were added, we observed a further PWV shift (Figure 1B). In initial experiments, we deliberately limited our examination of apoptotic cell interactions to apoptotic targets prepared from nonadherent cells so that we could examine interactions with control viable targets without the complication of further adhesion-related PWV shifts. We monitored changes in the apoptotic target-associated PWV kinetically. Whereas the addition of apoptotic targets led to an immediate increase in PWV over the adhesion-dependent PWV of responders alone in many instances, the most characteristic effect of apoptotic targets was a shift in the reflected resonant peak wavelength (ΔPWV) occurring 30–40 min after the addition of targets. Note that, in this case, the magnitude of $\Delta PWV_{interaction}$ is no greater than that of $\Delta PWV_{adhesion}$. We observed this relationship generally (e.g., also see Figure 2). The kinetics of target cell settling may contribute to the kinetic $\Delta PWV_{interaction}$ pattern we observe with apoptotic targets; we did not accelerate the movement of targets toward the responder monolayer by centrifugation (in order not disturb the biosensor surface, and also to capture the full time course of interactions). On the other hand, those kinetics may reflect cytoskeletal rearrangements that ensue in responder cells after their interaction with apoptotic targets (see later discussion of Figure 4D). (As is the case with $\Delta PWV_{adhesion}$, the observed $\Delta PWV_{interaction}$ is calculated for each well independently, subtracting the observed adhesion-dependent PWV from the PWV determinations made after apoptotic target addition.)

As seen in Figure 1B, the characteristic kinetic ΔPWV pattern reflects specifically the interaction of responder cells with apoptotic target cells. Viable target cells do not elicit this characteristic ΔPWV pattern, just as they fail to trigger immunomodulatory responses or bind to responder cells. In addition, neither apoptotic nor viable target cells alone interact significantly with the biosensor surface, as would be expected from the use of nonadherent cells as targets.

It is significant that this biosensor approach does not necessitate a washing step to remove unbound targets. In contrast to cytofluorimetric approaches (see later discussion of Figure 4) and our previous fluorescence-based microwell binding assay (Cocco and Ucker, 2001), the absence of such a step minimizes technical complications associated with the disruption of responder cell adhesion. We observed that the interaction of some cells (especially macrophages) with apoptotic targets results in a diminution of responder cell adhesion (see later discussion of Figure 5F; Cocco and Ucker, 2001); in these instances, the further disruption of adhesion with washing steps precludes any reliable analysis.

Finally, although the characteristic apoptotic $\Delta PWV_{interaction}$ pattern reflects specifically the interaction of responder cells with apoptotic target cells, it remains an important issue to assess whether $\Delta PWV_{interaction}$ is a direct measure of the actual binding of apoptotic targets or is some secondary consequence of apoptotic recognition,

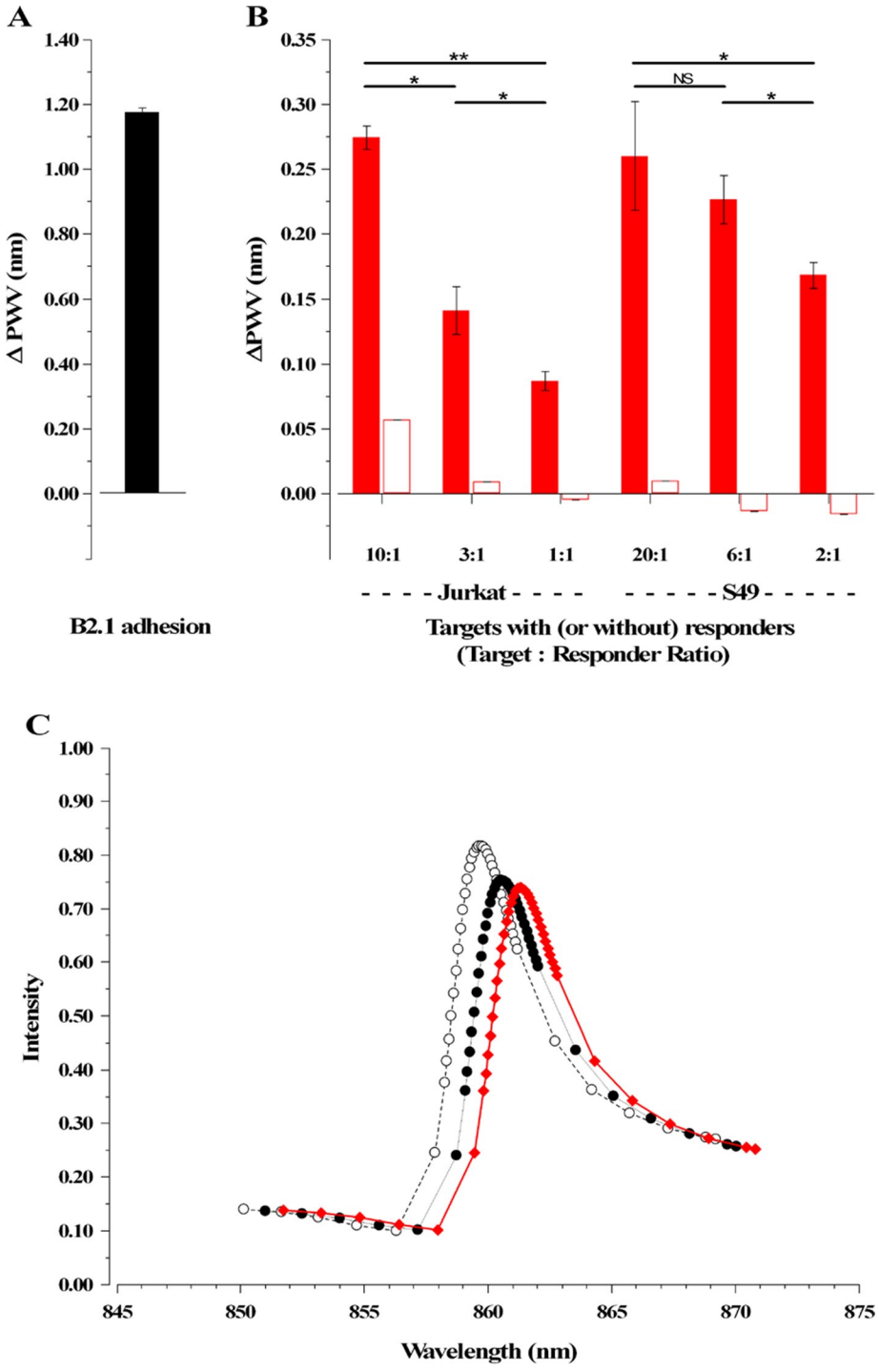

FIGURE 2: The characteristic resonant wavelength shift (ΔPWV) of apoptotic recognition depends on apoptotic target dose. A. The change in peak (reflected light) wavelength value (ΔPWV) associated with adhesion ($\Delta PWV_{adhesion}$) of human B2.1 responder cells to the biosensor surface of microwells was determined (■), as in Figure 1. Responder cells were plated 12 h earlier at 1×10^5 cells/well and incubated overnight at 37°C. Data are presented as the mean (±SEM) of triplicate determinations. (B) The interaction of apoptotic murine S49 and apoptotic human Jurkat T-lymphocyte target cells (apoptosis was induced by treatment with actinomycin D) with adherent B2.1 responder cells was monitored in biosensor microwells in which responder cells had been previously seeded (■), as well as in wells without B2.1 responders (□). Targets were added to wells at the indicated target:responder ratios. PWV readings were acquired 40 min after target cell addition. Data, analyzed as in Figure 1, are presented as the mean (±SEM) of triplicate determinations. (C) Single-well tracings of PWV determinations (reflected light intensity as a function of wavelength) of wells without cells (medium only; ○), with B2.1 responders alone (●), and with apoptotic Jurkat targets (apoptosis was induced by treatment with actinomycin D) with B2.1 responders (◆), representative of triplicate determinations. The experiment was repeated independently >10 times, except for experiments with S49 targets (in B), which were repeated three times. In A and B, differences of PWV values between wells with and without responder cells ($\Delta PWV_{adhesion}$) are significant ($p<0.001$; Student's two-tailed paired t-test), and differences of PWV values between wells with and without responder cells to which apoptotic target cells were added also are significant ($p < 0.001$; Student's two-tailed paired *t* test) in all cases. The statistical significance of differences of $\Delta PWV_{interaction}$ as a function of target dose, calculated by Student's two-tailed paired *t* test, is indicated (**$p < 0.01$; *$p < 0.1$; NS, $p > 0.1$). Differences between the three curves in C are highly significant ($p < 0.0001$; two-way ANOVA).

such as target cell phagocytosis. We explore this question in greater detail later (see Figure 4 later in this article).

The resonant wavelength shift of apoptotic interaction depends on the dose of apoptotic target cells

We examined the characteristic resonant wavelength shift (ΔPWV) of apoptotic recognition further by testing different apoptotic targets and varying the input of those targets added to wells in which a fixed number of responder cells had been plated previously. Again, we observed that the addition of apoptotic targets led to a PWV shift (Figure 2B) distinct from $\Delta PWV_{adhesion}$ (Figure 2A), with the characteristic kinetics (peak ΔPWV ~40 min after the addition of targets) shown in Figure 1B. Of importance, this effect was not limited to a particular population of apoptotic targets.

The magnitude of the apoptotic recognition-specific PWV shift is decidedly dependent on the dose of added apoptotic cells. As shown in Figure 2B, higher numbers of apoptotic targets per responder (higher target:responder ratios) elicited greater PWV shifts, and the response as a function of target dose, over a range of one order of magnitude, was essentially linear. Again, neither viable target cells (unpublished data) nor apoptotic targets in the absence of responders (Figure 2B) elicited this characteristic ΔPWV effect. In this experiment, the magnitude of $\Delta PWV_{adhesion}$ (Figure 2A) is greater than that of $\Delta PWV_{interaction}$ (Figure 2B). As noted earlier (see Figure 1), we found generally that the magnitude of $\Delta PWV_{interaction}$ is not greater than that of $\Delta PWV_{adhesion}$. Although variation among independent replicates within a single experiment is minimal (the SEMs were less than ±0.05 nm in all

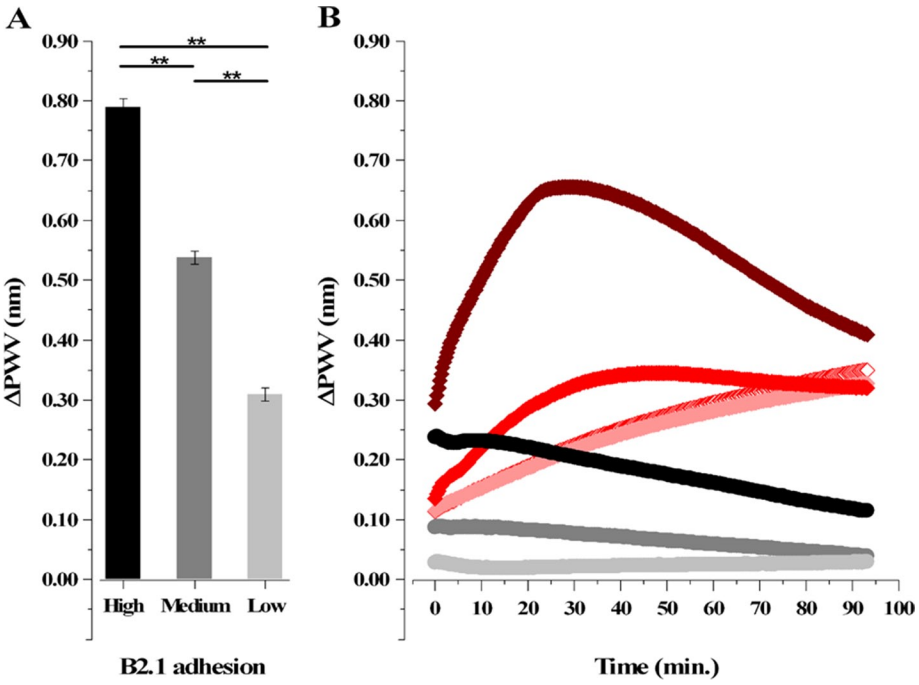

FIGURE 3: The characteristic resonant wavelength shift (ΔPWV) of apoptotic recognition depends on viable responder cell dose. (A) The change in peak (reflected light) wavelength value (ΔPWV) associated with adhesion ($\Delta PWV_{adhesion}$) of human B2.1 to the biosensor responder cells surface of microwells was determined as in Figure 1. Here responder cells were plated 12 h earlier at different densities (1×10^5 [high, ■], 3×10^4 [medium, ■], and 1×10^4 cells/well [low, ■]) and incubated overnight at 37°C. Data are presented as the mean (±SEM) of triplicate determinations. (B) The interaction of apoptotic human Jurkat T-lymphocyte target cells (apoptosis was induced by treatment with actinomycin D) with the adherent B2.1 responder cells was monitored in biosensor microwells in which responder cells had been plated previously at different densities (high, ◆; medium, ◆; low, ◆), as well as in wells without B2.1 responders (◇). Targets (3×10^5 cells/well; note that corresponding target:responder ratio varies from 3:1 to 30:1) were added to wells, and data acquisition was begun immediately, as in Figure 1. ΔPWV determinations also were made in the absence of targets for B2.1 responders plated at different densities as earlier (high, ●; medium, ●; and low, ●). The data presented are the means of triplicate single-well determinations. SEMs are less than ±0.05 nm in all cases; for clarity, SEMs are not shown. The experiment was repeated independently three times. In A, differences of PWV values between wells with and without responder cells ($\Delta PWV_{adhesion}$) are significant ($p < 0.001$; Student's two-tailed paired *t* test). The statistical significance of differences of $\Delta PWV_{adhesion}$ as a function of responder cell dose, calculated by Student's two-tailed paired *t* test, is indicated (**$p < 0.01$). In B, differences of PWV values between wells with responder cells at high and medium cell densities to which apoptotic target cells were added, compared with wells with targets alone (without responder cells), are significant ($p < 0.0001$; two-way ANOVA). Differences between wells with responder cells at low cell density to which apoptotic target cells were added, compared with wells with targets alone, are not significant ($p > 0.1$; two-way ANOVA).

cases), we do find that the magnitudes, but not the kinetics, of PWV changes vary significantly between independent experiments performed on separate days (e.g., compare Figures 1 and 2). We do not know the basis of this variability.

This experiment, as well as experiments with other cell lines (see later discussion of Figures 4B and 5D), confirms the species-unrestricted (evolutionarily conserved—one of the SUPER criteria; Ucker *et al.*, 2012) nature of apoptotic recognition (Cvetanovic *et al.*, 2006). Here apoptotic targets of disparate species (S49 is an immature murine thymoma cell line, and Jurkat is a mature human T-cell leukemia cell line) exhibit comparable extents of binding to responder cells and elicit equivalent PWV shifts (Figure 2B).

The data in Figure 2C document the resonant reflected light spectra obtained with the biosensors, from which peak wavelength values are determined, and exemplify the PWV shifts associated with adhesion and apoptotic recognition. In contrast to the peak wavelength values, the shape of these spectra, which is a function of the resonance properties of the biosensor itself, is constant and independent of incubation condition. This is expected for adsorption of biomaterial that modifies only the real part of the refractive index within the evanescent field region without introducing material that partially absorbs the resonant wavelength of ~860 nm.

The resonant wavelength shift of apoptotic interaction depends on the dose of viable responder cells

We further examined the characteristic resonant wavelength shift (ΔPWV) of apoptotic recognition as a function of responder cell dose by varying the number of responder cells plated in biosensor wells. Again, we observed that the addition of apoptotic targets led to a PWV shift (Figure 3B) distinct from and of lesser magnitude than $\Delta PWV_{adhesion}$ (Figure 3A), with characteristic kinetics. In contrast to the titration of targets, a sensitivity threshold for this methodology was quickly reached in the titration of responders.

The magnitudes of both the adhesion-specific and the apoptotic recognition–specific PWV shifts are dependent on the dose of responder cells. As evident here (Figure 3B) and noted earlier (Figure 1), nonadherent target cells alone do not interact significantly with the biosensor surface. However, that small background signal is substantial relative to the small ΔPWV associated with low responder cell density (Figure 3B). On the other end of the range, adherent responders became overconfluent and lost adhesion if plated at too high a density (unpublished data). Collectively the data reveal that the efficacy of this biosensor methodology depends on a reasonably robust, well-adhered responder monolayer within a relatively narrow density range. This conclusion underscores the need for responder adhesion and associated cytoskeletal plasticity (see later discussion of Figures 4 and 5).

The resonant wavelength shift of apoptotic interaction depends on cytoskeletal rearrangement and is independent of phagocytosis

The data thus far demonstrate that the characteristic apoptotic $\Delta PWV_{interaction}$ pattern reflects specifically the dosage-dependent interaction of responder cells with apoptotic target cells. To test whether $\Delta PWV_{interaction}$ is a direct readout of actual binding, we asked whether $\Delta PWV_{interaction}$ could be dissociated from secondary consequences of apoptotic recognition.

As a first step, we explored one closely linked consequence of recognition, phagocytosis. The data of Figures 1–3, which involve

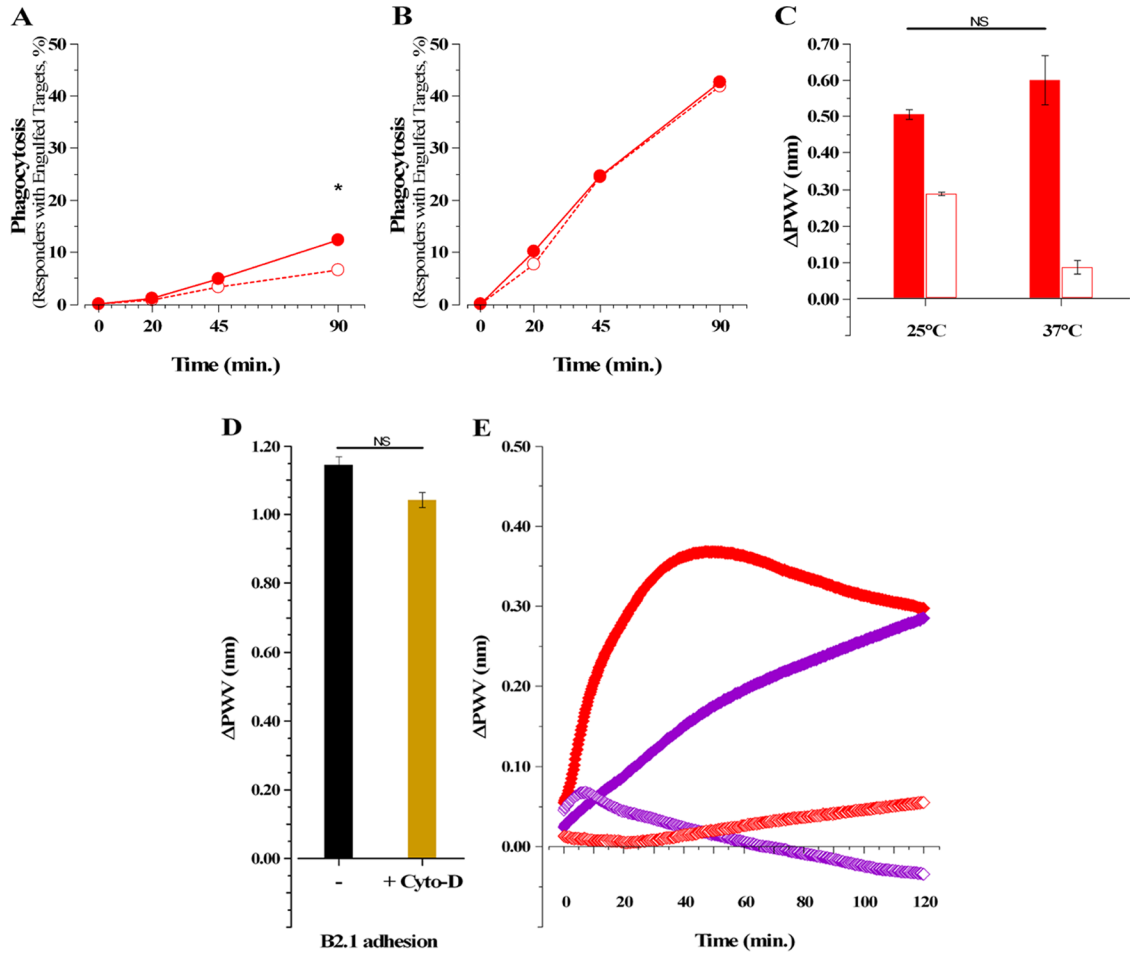

FIGURE 4: The characteristic resonant wavelength shift (ΔPWV) of apoptotic recognition depends on cytoskeletal rearrangement but is independent of phagocytosis. Phagocytosis of apoptotic target cells (human Jurkat T-lymphocytes induced to die by treatment with actinomycin D) by human B2.1 responder cells (A) and ANA-1 murine macrophages (B) at 25°C (○) and 37°C (●) was assessed kinetically. Targets were incubated with responders at a target to responder ratio of 6:1. The compiled results of cytofluorimetric analyses are presented here. (C) The change in peak (reflected light) wavelength value (ΔPWV) associated with the interaction of those apoptotic Jurkat T-lymphocytes with adherent B2.1 responder cells ($\Delta PWV_{interaction}$) was monitored in biosensor microwells in which responder cells had been previously seeded (□), as well as in wells without B2.1 responders (■). Responder cells were plated 12 h earlier at 1×10^5 cells/well and incubated overnight at 37°C. Targets were added to wells at a target to responder ratio of 10:1, and PWV readings were acquired 40 min after target cell addition. Data, analyzed as in Figure 1, are presented as the mean (±SEM) of triplicate determinations. (D) Change in peak (reflected light) wavelength value (ΔPWV) associated with adhesion ($\Delta PWV_{adhesion}$) of human B2.1 responder cells to the biosensor surface of microwells was determined as in Figure 1. Responder cells were plated 12 h earlier at 1×10^5 cells/well and incubated overnight at 37°C. Responders then were treated with cytochalasin D (2 μM; ■) or left untreated (■) for an additional 45 min at 37°C. Data are presented as the mean (±SEM) of triplicate determinations. (E) The interaction of apoptotic Jurkat target cells (again, apoptosis was induced by treatment with staurosporine) with adherent B2.1 responder cells was monitored in biosensor microwells in which responder cells had been previously seeded (◆◆), as well as in wells without B2.1 responders (◇◇). Targets (1×10^6 cells/well; target:responder ratio, 10:1) were added to wells in the presence (◆◇) or absence (◆◇) of cytochalasin D, and data acquisition was begun immediately, as in Figure 1. The data presented are the means of triplicate single-well determinations. SEMs are less than ± 0.05 nm in all cases; for clarity, SEMs are not shown. Differences in the extent of phagocytosis as a function of temperature (A, B) were not significant except at 90 min for B2.1 cells (A), as indicated (*$p < 0.1$; Student's two-tailed paired *t* test). In C, differences of PWV values between wells with and without responder cells to which apoptotic target cells were added are significant ($p < 0.001$; Student's two-tailed paired *t* test). The statistical insignificance of differences of $\Delta PWV_{interaction}$ as a function of target dose, calculated by Student's two-tailed paired *t* test, is indicated (NS: $p > 0.1$). The experiment in D and E was repeated independently three times. In D, differences of PWV values between wells with and without responder cells ($\Delta PWV_{adhesion}$) are significant ($p < 0.001$; Student's two-tailed paired *t* test). The statistical insignificance of differences of $\Delta PWV_{adhesion}$ as a function of cytochalasin D treatment, calculated by Student's two-tailed paired *t* test, is indicated (NS: $p > 0.1$). In E, differences of PWV values between wells with responder cells to which apoptotic targets were added ($\Delta PWV_{interaction}$) in the absence and in the presence of cytochalasin D, as well as differences between corresponding wells with and without responder cells to which target cells were added, are highly significant ($p < 0.0001$; two-way ANOVA).

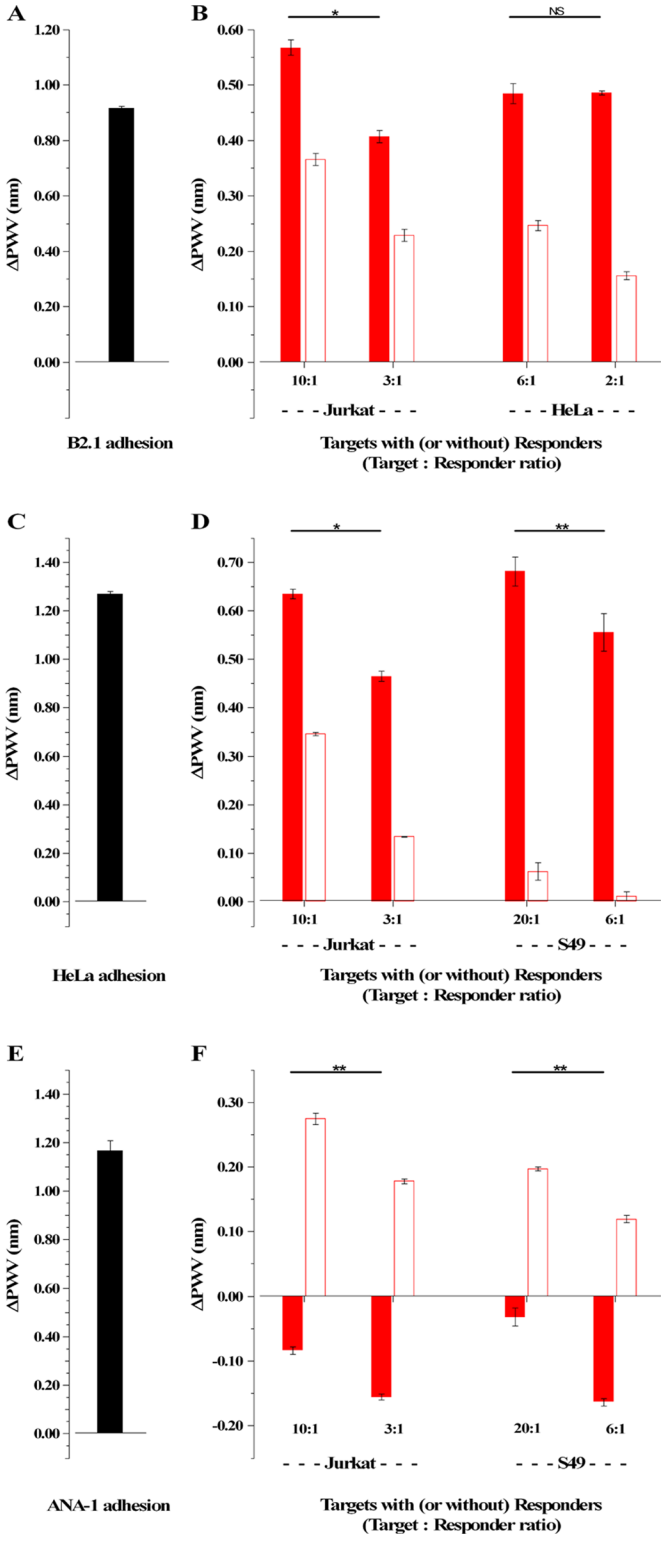

FIGURE 5: The characteristic resonant wavelength shift (ΔPWV) of apoptotic recognition is observed with a variety of responder and target cells. (A) The change in peak (reflected light) wavelength value (ΔPWV) associated with adhesion ($\Delta PWV_{adhesion}$) of human B2.1 responder cells to the biosensor surface of microwells was determined (■) as in Figure 1. Responder cells were plated 12 h earlier at 1×10^5 cells/well and incubated overnight at 37°C. Data are presented as the mean (±SEM) of triplicate determinations. (B) The interaction of apoptotic human Jurkat T-lymphocyte and HeLa epithelial target cells (apoptosis was induced by treatment with actinomycin D in both cases) with adherent B2.1 responder cells was monitored in biosensor microwells in which responder cells had been previously seeded (□), as well as in wells without B2.1 responders (■). Targets were added to wells at the indicated target:responder ratio. PWV readings were acquired 40 min after target cell addition. Data, analyzed as in Figure 1, are presented as the mean (±SEM) of triplicate determinations. Correspondingly, the $\Delta PWV_{adhesion}$ of (viable) HeLa cells plated 12 h earlier at 1×10^5 cells/well and incubated overnight at 37°C (C), and the $\Delta PWV_{interaction}$ of those cells as responders 40 min after addition of apoptotic human Jurkat and apoptotic murine S49 targets (D; apoptosis was induced by treatment with actinomycin D in both cases), was determined. Finally, the $\Delta PWV_{adhesion}$ of murine ANA-1 macrophages plated 12 h earlier at 1×10^5 cells/well and incubated overnight at 37°C (E) and the $\Delta PWV_{interaction}$ of those cells with apoptotic Jurkat and apoptotic S49 targets (F; apoptosis was induced by treatment with actinomycin D in both cases) was determined similarly. The complete experiment was repeated independently three times. Differences of PWV values between wells with and without responder cells ($\Delta PWV_{adhesion}$) are significant ($p < 0.001$; Student's two-tailed paired *t* test), and differences of PWV values between wells with and without responder cells to which apoptotic target cells were added also are significant ($p < 0.001$; Student's two-tailed paired *t* test) in all cases. The statistical significance of differences of $\Delta PWV_{interaction}$ as a function of target dose, calculated by Student's two-tailed paired *t* test, is indicated (**$p < 0.01$; *$p < 0.1$; NS, $p > 0.1$).

apoptotic target cell interactions with B2.1 responders—minimally phagocytic cells derived from a transformed human kidney epithelial cell line—already suggest that phagocytosis likely is not involved. We probed this issue more rigorously by quantifying the extent of target cell phagocytosis and manipulating conditions to alter phagocytosis specifically.

We assessed the phagocytosis of apoptotic human target cells by B2.1 responder cells objectively with a cytofluorimetric assay (Cvetanovic and Ucker, 2004). As shown in Figure 4A, the extent of phagocytosis during the first few minutes of incubation of targets and responders, especially at 25°C, is very low. (For context, compare the extents of phagocytosis of human apoptotic targets by human B2.1 cells and by cells of the phagocytic murine macrophage cell line ANA-1; Figure 4B.) Essentially, <5% of B2.1 responder cells have engulfed targets when the $\Delta PWV_{interaction}$ is maximal. Still, it could be that those few phagocytically active responders account entirely for the $\Delta PWV_{interaction}$ signal. Previously we showed that the extent of phagocytosis, but not of recognition, was temperature dependent (Cocco and Ucker, 2001), especially for nonprofessional phagocytes. We took advantage of those findings to ask whether the characteristic apoptotic $\Delta PWV_{interaction}$ pattern was sensitive to incubation temperature. Indeed, whereas roughly twice as many B2.1 responders ultimately engulf targets at 37°C as at 25°C (Figure 4A), the magnitude and the kinetics of the PWV shifts observed with the biosensor (Figure 4C and unpublished data) are not altered. More generally, it is significant that, while the extent of phagocytosis increases with incubation time, the interaction-specific PWV shifts decay with extended time. Although a contribution to $\Delta PWV_{interaction}$ by phagocytosis cannot be excluded, these data suggest that phagocytosis does not contribute appreciably to the ΔPWV signal. We conclude that $\Delta PWV_{interaction}$ is primarily a measure of recognition and not of phagocytosis.

Because we observed slight alterations in responder cell morphology associated with apoptotic cell binding, we wondered whether $\Delta PWV_{interaction}$ might be a consequence of other cytoskeletal rearrangements associated with recognition. Pharmacological

agents that affect cytoskeletal rearrangements interfere with phagocytosis, of course, but they do not abrogate apoptotic cell recognition and the immunological responses elicited by that recognition (Reddy *et al.*, 2002; Cvetanovic and Ucker, 2004). Having excluded a substantial role for phagocytosis in $\Delta PWV_{interaction}$, we were able to ask whether cytoskeletal rearrangements, independent of engulfment, might contribute to the biosensor signal.

We examined the involvement of actin microfilaments by treating responder cells with cytochalasin D, an inhibitor of actin polymerization. Cytochalasin D did not interrupt established adhesion-dependent ΔPWV (Figure 4D), but it did interfere with recognition-dependent ΔPWV (Figure 4E). Intriguingly, whereas the relatively rapid PWV shift characteristic of the recognition of apoptotic cells by responder cells is abolished by cytochalasin D treatment, a slower and apparently actin-independent PWV shift is evident. That cytochalasin D abolishes characteristic target-specific ΔPWV but does not interfere with functional recognition (Cvetanovic and Ucker, 2004) suggests that cytoskeletal rearrangements and the measurable ΔPWV associated with apoptotic target interaction are proximal and dissociable consequences of recognition. Independent experiments evaluating necrotic target interactions (see later discussion of Figure 6) lead to a similar conclusion.

It could be that cytoskeletal rearrangements associated with the recognition of apoptotic cells are involved in regulating responder cell adhesion. Whereas adhesive interactions are enhanced in some cells after their interaction with apoptotic targets, adhesion is diminished in other cells (especially macrophages) after apoptotic cell binding (see next subsection; Cocco and Ucker, 2001). In summary, our data demonstrate that the apoptotic $\Delta PWV_{interaction}$ is a specific readout of the recognition by responder cells of apoptotic target cells, dependent on (dissociable) cytoskeletal rearrangements but independent of target cell phagocytosis.

The characteristic resonant wavelength shift of apoptotic interaction is observed with a variety of responder and target cells

We showed that the recognition of apoptotic targets with respect to functional immunological outcomes (Cvetanovic *et al.*, 2006), phagocytosis (Figure 4B), and $\Delta PWV_{interaction}$ (Figures 2B and 5D) exhibits no species restriction (i.e., apoptotic determinants for recognition are evolutionarily conserved, one of the SUPER criteria; Ucker *et al.*, 2012). Functionally, we also showed that apoptotic cells derived from different tissues of origin trigger similar modulatory responses (Cvetanovic *et al.*, 2006). We asked whether targets derived from different tissues also elicit similar $\Delta PWV_{interaction}$. The data in Figure 5B confirm that apoptotic recognition determinants are expressed ubiquitously (ubiquitously expressed is another of the SUPER criteria; Ucker *et al.*, 2012) on apoptotic target cells of different tissue types. Here apoptotic targets of lymphoid (Jurkat is a mature human T-cell leukemia cell line) and epithelial (HeLa is a human cervical carcinoma cell line) origins elicit comparable PWV shifts (Figure 5B). Note that equal $\Delta PWV_{interaction}$ signals are induced by interaction with fewer of the much larger apoptotic HeLa cells (~20 µm diameter) relative to apoptotic Jurkat targets (~7 µm diameter).

Viable nonadherent targets do not bind to responder cells (Cocco and Ucker, 2001) and do not trigger $\Delta PWV_{interaction}$ (Figure 1). However, we were not able to examine the behavior of viable adherent targets (such as HeLa cells) in this context because their adhesion to the biosensor surface and the associated $\Delta PWV_{adhesion}$ confound the evaluation of $\Delta PWV_{interaction}$.

We also showed previously that the ability to recognize and respond to apoptotic cells is a property ubiquitous among professional and nonprofessional phagocytes, as well as nonphagocytic cell types. We wondered whether adherent cell lines and cell types other than B2.1 also would yield comparable $\Delta PWV_{interaction}$ signals. As a first test, we examined HeLa cells as responders, with apoptotic lymphoid targets. The data in Figure 5, C and D, reveal the equivalent $\Delta PWV_{adhesion}$ and $\Delta PWV_{interaction}$ signals observed with these responders. We observed analogous $\Delta PWV_{interaction}$ signals when viable HeLa responders interact with apoptotic HeLa targets, and we also observed comparable signals with other adherent cell lines, including primary mouse embryo fibroblasts (unpublished data).

The behavior of macrophage responders in this setting is unusual. The data in Figure 5, E and F, are exemplary and represent experiments with cells of one murine macrophage cell line, ANA-1. Whereas $\Delta PWV_{adhesion}$ is not different from epithelial or fibroblastic cells, apoptotic target interactions lead to the profound loss of macrophage adhesion (indicated by the reversal of $\Delta PWV_{adhesion}$ and confirmed microscopically). Other macrophage cell lines and primary elicited murine macrophages behave similarly (unpublished data).

Interference with cytoskeletal rearrangement (Figure 4, C and D) or loss of adhesion of some (especially macrophage) responders (Cocco and Ucker, 2001) after their interaction with apoptotic targets precludes the analysis of binding. The data in Figure 5F show unambiguously that target interactions lead to the loss of adhesion of responding macrophages. Our previous misinterpretation of the

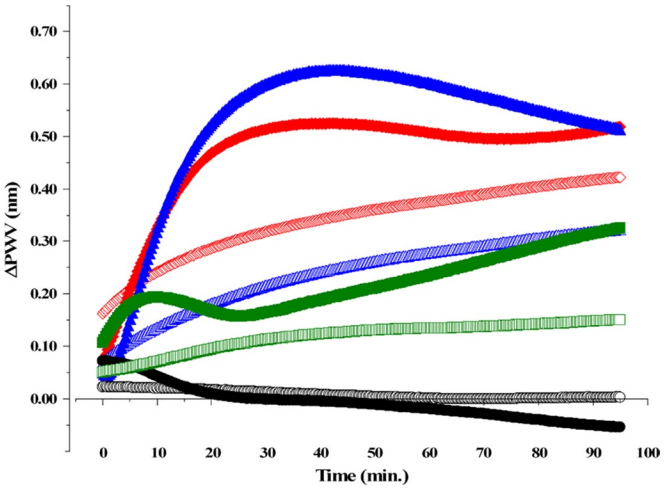

FIGURE 6: Necrotic and apoptotic targets trigger a similar resonant wavelength shift (ΔPWV). The interaction of apoptotic (◆◇), necrotic (▲△), and viable (■□) Jurkat target cells (apoptosis was induced by treatment with actinomycin D) with B2.1 responder cells was monitored in biosensor microwells in which responder cells had been plated 12 h earlier (◆▲■; 1×10^5 cells/well; 37°C), as well as in wells without B2.1 responders (◇△□). Targets (1×10^6 cells/well, target:responder ratio of 10: 1) were added to wells, and data acquisition was begun immediately, as in Figure 1. The data presented are the means of triplicate single-well determinations. ΔPWV determinations also were made in the absence of targets for B2.1 responders (●) and in the absence of cells (medium only; ○). SEMs are less than ±0.05 nm in all cases; for clarity, SEMs are not shown. The experiment was repeated independently nine times. Differences of PWV values between wells with responder cells to which targets were added ($\Delta PWV_{interaction}$) or to which target cells were not added are highly significant ($p < 0.0001$; two-way ANOVA). Differences of PWV values between wells with responder cells to which apoptotic, necrotic, or viable targets were added also are highly significant ($p < 0.0001$; two-way ANOVA).

discrimination of targets by macrophages (Cocco and Ucker, 2001) was due to this loss of adhesion and the consequent failure of the fluorescence plate reader assay used. Here the loss of adhesion, although still a technical limitation, is documented by an unequivocal readout.

A resonant wavelength shift of interaction also is observed with necrotic target cells

Cells that die pathologically (that is, a "necrotic" vs. an "apoptotic" death) also are recognized by responder cells but do not modulate inflammatory responses (Cocco and Ucker, 2001; Cvetanovic and Ucker, 2004; Cvetanovic *et al.*, 2006). The recognition of these two classes of dying cells proceeds to comparable extents, albeit via distinct and noncompeting processes (Cocco and Ucker, 2001; Patel *et al.*, 2006). Our earlier experiments with cytochalasin D (Figure 4E) indicated that $\Delta PWV_{interaction}$ reflects a proximal recognition event and is dissociable from immunomodulatory consequences of recognition. We used necrotic targets to test independently whether target cell binding per se, unconnected to the immunomodulatory consequences triggered by apoptotic target recognition, would elicit a $\Delta PWV_{interaction}$ signal.

As shown in Figure 6, necrotic targets elicit a PWV shift very similar in pattern and magnitude to that triggered by apoptotic targets. Again, using nonadherent cells as targets, we find that necrotic targets alone, like apoptotic and viable target cells, do not interact significantly with the biosensor surface. This characteristic kinetic $\Delta PWV_{interaction}$ pattern, then, reflects proximal events of interaction of responder cells with dead target cells.

The $\Delta PWV_{interaction}$ for necrotic targets also is dependent on target cell dose (unpublished data), as is the case for $\Delta PWV_{interaction}$ of apoptotic targets (Figure 2B). Macrophage responders also lose adhesion after interaction with necrotic targets (unpublished data), as they do with apoptotic targets (Figure 5F).

DISCUSSION

Here we report a novel and sensitive method for real-time detection specifically of apoptotic target cell recognition by viable responder cells. The approach we describe involves photonic crystal biosensors and takes advantage of alterations in the adhesive interactions of responder cells with the biosensor surface after responder cell recognition of targets. Target cells neither adhere to nor interact appreciably with the biosensor surface. We observe discrete, dose-dependent spectral shifts (ΔPWV) reflective of the binding by adherent viable responder cells of (nonadherent) apoptotic target cells ($\Delta PWV_{interaction}$) distinct from responder cell adhesion–specific ΔPWV ($\Delta PWV_{adhesion}$). In this sense, the method reflects events distal to the biosensor surface. Nonetheless, these readouts reflect events proximal to cellular recognition.

Of importance, the events triggering $\Delta PWV_{interaction}$ are distinct and dissociable from subsequent responses leading to immunomodulatory transcriptional regulation. We arrive at this conclusion from several independent observations. Of most significance, interference with microfilament dynamics in responder cells disrupts the ΔPWV signal resulting from apoptotic target interactions but does not interfere with immunomodulatory transcriptional responses. Moreover, in macrophages, where target cell recognition induces a loss of responder cell adhesion (precluding the detection of any $\Delta PWV_{interaction}$ signal), robust transcriptional responses ensue after apoptotic target recognition. Finally, whereas the $\Delta PWV_{interaction}$ signal for necrotic target cell interaction is equivalent to that for apoptotic targets, necrotic targets do not trigger immunomodulatory transcriptional responses.

On the other hand, $\Delta PWV_{interaction}$ is a reflection of early events associated with target cell recognition and binding. Consistent with previous binding studies, the $\Delta PWV_{interaction}$ readout indicates that apoptotic target recognition ensues rapidly, even at reduced temperatures. Our data also demonstrate that $\Delta PWV_{interaction}$ is linked to obligate cytoskeletal changes in responder cells that result in enhanced (or weakened) adhesion, although apoptotic cell phagocytosis is not involved. Although intervening signaling steps between putative receptors for apoptotic recognition determinants and cytoskeletal reorganization must be involved, such steps are as yet uncharacterized. Consequently, $\Delta PWV_{interaction}$ is the most proximal specific measure of apoptotic recognition available.

Whereas differences among primary cells and established cell lines of a particular cell type are insubstantial, it is worth noting that not all responder cell types exhibit characteristic $\Delta PWV_{interaction}$. Technically, the methodology is limited to adherent responders that maintain adhesion throughout their interaction with target cells. Macrophages, in particular, do not meet this requirement and do not work in this assay, although they do recognize apoptotic cells (Cvetanovic and Ucker, 2004). Data here (Figure 5F), which document the loss of macrophage adhesion after target interaction, serve to explain definitively earlier observations that were taken to suggest an absence of target interaction (Cocco and Ucker, 2001). The methodology also is limited to nonadherent target cells. In fact, this poses no real limitation, since dead cells are, of course, nonadherent.

The utility of this binding assay derives from the specific readout it affords of early events of apoptotic target recognition and the relatively gentle conditions under which those interactions can be assessed. Just as the loss of responder cell adhesion precludes the analysis of target cell interactions, as discussed earlier, so too is the disturbance of weak and disruptable interactions between responders and targets problematic. The absence of washing steps in the assessment of target:responder interactions is a decided advantage of this biosensor methodology. Although the characteristic shape and kinetics of $\Delta PWV_{interaction}$ are reliable indicators of target interactions, variation in the magnitude of $\Delta PWV_{interaction}$ between experiments is puzzling. An important technical goal is to improve the consistency of this signal. Independently, the further development of this approach in combination with microscopic imaging (photonic crystal enhanced microscopy; Lidstone *et al.*, 2011; Chen *et al.*, 2013) may advance the dissection of target cell interactions by facilitating analysis on the level of single responder cells.

The validity of the photonic crystal biosensor assessment of apoptotic recognition, on one level, is reinforced by the fact that the results obtained are consistent with results from our previous work, including both direct and indirect measures of recognition. In this context, the biosensor measurements provide independent confirmation of the striking species-unrestricted and ubiquitous nature of apoptotic recognition. This approach also has provided new insights to this process. We find that recognition leads to dissociable cytoskeletal events, as well as to immunological responses. We speculate that proximal signaling signatures linking apoptotic recognition and cytoskeletal reorganization will contribute to the identification of functional receptors for apoptotic recognition determinants. Of interest, titration experiments (see, especially, Figure 3B) suggest that $\Delta PWV_{interaction}$ is saturable, raising the possibility that biochemical characteristics of binding (especially equilibrium constants, etc.) might be gleaned from the biosensor data. The extent to which all responder cells in a population manifest target cell binding is not established from these experiments. It will be important to determine whether

$\Delta PWV_{interaction}$ represents the homogeneous interaction of all responder cells in a well or, instead, the response of only some cells. Experimental conditions under which $\Delta PWV_{interaction}$ is assessed always involve excess target cells per responder, so it is probabilistically possible that interactions involve all responders. On the other hand, we noted previously that great heterogeneity exists with regard to target cell phagocytosis among phagocytic responders (the "jackpot" phenomenon; Cocco and Ucker, 2001). Here, too, combined imaging and biosensor analyses may help to provide absolute quantification of the $\Delta PWV_{interaction}$ signal and target cell binding.

Most practically, the photonic crystal methodology, as a straightforward and objective readout of proximal events of apoptotic recognition, offers a potential screening approach with which to identify antibodies or other molecular probes of apoptotic recognition determinants. This will be of great value in the dissection of the early recognition events associated with IAI and immunosuppression. For example, functional testing of the externalized glycolytic enzyme molecules, among candidate apoptotic recognition molecules meeting SUPER criteria (Ucker *et al*., 2012), is of intense interest.

MATERIALS AND METHODS

Cells and cell culture

S49 murine thymoma cells, ANA-1 murine macrophages, and Jurkat human T-cell leukemia cells were cultured at 37°C in a humidified 5% (vol/vol) CO_2 atmosphere in RPMI 1640 medium (Mediatech, Herndon, VA) supplemented with heat-inactivated 10% (vol/vol) fetal bovine serum (FBS; HyClone Laboratories, Logan, UT), 2 mM L-glutamine, and 50 µM 2-mercaptoethanol. HeLa human cervical carcinoma cells and B2.1 cells, a stable NFκB-luciferase transfectant reporter clone of 293T human transformed kidney epithelial cells (Cvetanovic *et al*., 2006), and parental 293T cells were grown in DMEM with 4.5 g/l glucose (Mediatech) supplemented with 10% (vol/vol) FBS and 2 mM L-glutamine (Mediatech). As noted later (*Photonic crystal biosensor assays*), media were supplemented with 4-(2-hydroxyethyl)-1-piperazineethanesulfonic acid (HEPES) buffer in some cases.

Induction of apoptotic and necrotic death

Physiological cell death (apoptosis) was induced by treatment of cells with the macromolecular synthesis inhibitor actinomycin D (200 ng/ml, 12 h) or the protein kinase inhibitor staurosporine (1 µM in serum-free medium, 3 h). Pathological cell death (necrosis) was triggered by incubation of cells at 56°C for 20 min (until trypan blue uptake indicated compromise of membrane integrity). We described the cytofluorimetric profiles of these dead cells previously (Cocco and Ucker, 2001). In all cases, target cells (viable, apoptotic, and necrotic cells) were washed four times in complete media and resuspended in the medium of the responder cells to be tested.

Photonic crystal biosensor assays

Titanium dioxide–coated photonic crystal 96-well biosensor plates and the SRU BIND EXPLORER plate reader (SRU Biosystems, Woburn, MA) were used in these experiments. Wells were washed extensively in the complete medium of responder cells, supplemented with HEPES buffer (pH 7.4; 10 mM), and incubated with 100 µl of that medium. The initial PWV of reflected light for each well was measured. Responder cells at respective concentrations then were added to wells in another 100 µl of the responder cell medium, supplemented with HEPES buffer (pH 7.4; 10 mM). Responder cells were allowed to adhere overnight at 37°C. Then responder adhesion–specific PWV was measured. Finally, target cells were added to respective wells at desired concentrations in 50 µl of the responder cell medium, supplemented with HEPES buffer (pH 7.4; 10 mM). Interaction-specific PWV was acquired subsequently in real time. ΔPWV was calculated specifically for each well with respect to previous readings of the same well. At least three replicates of each experimental condition were acquired in a single experiment; SEMs were less than ±0.05 nm in all cases. Most readings were acquired at 25°C; some experiments involved equilibrating the reader at a different temperature and acquiring data at that temperature. Note that the BIND instrument was not maintained in a 5% CO_2 environment, and all media used in biosensor experiments were supplemented with HEPES buffer (pH 7.4; 10 mM).

Cytofluorimetric analysis of phagocytosis

Phagocytosis was assessed as previously described (Cvetanovic and Ucker, 2004). Target cells were labeled green with 5(6)-carboxyfluorescein diacetate succinimidyl ester (CFDA; 0.2 µM; Molecular Probes, Eugene, OR) and washed extensively and then were induced to undergo apoptotic cell death, killed pathologically by heat treatment, or left untreated. Responder cells were labeled red with the tracking dye CMPTX (2 µM; Molecular Probes), washed extensively, and incubated overnight before coculture with apoptotic target cells. Responder cells then were washed with PBS, followed by a wash with PBS supplemented with 0.4 mM Na_2EDTA, followed by a wash with 0.05% trypsin-EDTA (Mediatech) to remove any bound targets. Cells then were gently lifted by scraping, and analyzed cytofluorimetrically on the BD LSR Fortessa (BD Biosciences, Franklin Lakes, NJ). Bound targets that that had not been engulfed did not remain adherent during these procedures. Cells that stained positively for CMPTX ($Ex\lambda = 577$ nm; $Em\lambda = 602 \pm 15$ nm) and also were CFDA positive ($Ex\lambda = 488$ nm; $Em\lambda = 530 \pm 15$ nm) represented responders that had engulfed targets. Phagocytosis is represented as the fraction of responder cells that are $CFDA^+$.

Statistical analysis

All experiments were repeated independently at least three times; the number of independent repetitions for any one experiment is indicated in the figure legends. Within any single repetition, triplicate replicates of each condition were performed. Data presented represent the mean (±SEM) of triplicates from a single representative repetition. All data were subjected to statistical analyses, either two-way analysis of variance (ANOVA) or Student's two-tailed paired *t* test as appropriate, using Prism software (GraphPad, La Jolla, CA). Differences of PWV values between wells with and without responder cells ($\Delta PWV_{adhesion}$) are significant ($p < 0.001$) in all cases. Similarly, differences of PWV values between wells with and without responder cells to which apoptotic or necrotic target cells were added are significant ($p < 0.01$) in all cases. Levels of statistical significance in other cases are indicated in the figures: $^{**}p < 0.01$, $^{*}p < 0.1$; NS, comparisons that are not statistically significant ($p > 0.1$).

ACKNOWLEDGMENTS

We gratefully acknowledge a pilot grant from the University of Illinois Cancer Center, which enabled this work. E.A.L. was funded by National Science Foundation Grant 0965918 (Integrative Graduate Education and Research Traineeship "Training the Next Generation of Researchers in Cellular and Molecular Mechanics and BioNanotechnology"). Additional support came from National Institutes of Health Grant AG029633 to D.S.U. We thank Brian Kay (University of Illinois at Chicago) for making his BIND reader available to us.

REFERENCES

Arur S, Uche UE, Rezaul K, Fong M, Scranton V, Cowan AE, Mohler W, Han DK (2003). Annexin I is an endogenous ligand that mediates apoptotic cell engulfment. Dev Cell 4, 587–598.

Birge RB, Ucker DS (2008). Innate apoptotic immunity: the calming touch of death. Cell Death Differ 15, 1096–1102.

Chan LL, Gosangari SL, Watkin KL, Cunningham BT (2007). A label-free photonic crystal biosensor imaging method for detection of cancer cell cytotoxicity and proliferation. Apoptosis 12, 1061–1068.

Chen W, Long KD, Lu M, Chaudhery V, Yu H, Choi JS, Polans J, Zhuo Y, Harley BA, Cunningham BT (2013). Photonic crystal enhanced microscopy for imaging of live cell adhesion. Analyst 138, 5886–5894.

Chung EY, Liu J, Homma Y, Zhang Y, Brendolan A, Saggese M, Han J, Silverstein R, Selleri L, Ma X (2007). Interleukin-10 expression in macrophages during phagocytosis of apoptotic cells is mediated by homeodomain proteins Pbx1 and Prep-1. Immunity 27, 952–964.

Cocco RE, Ucker DS (2001). Distinct modes of macrophage recognition for apoptotic and necrotic cells are not specified exclusively by phosphatidylserine exposure. Mol Biol Cell 12, 919–930.

Cunningham BT, Li P, Schulz S, Lin B, Baird C, Gerstenmaier J, Genick C, Wang F, Fine E, Laing L (2004). Label-free assays on the BIND system. J Biomol Screen 9, 481–490.

Cvetanovic M, Mitchell JE, Patel V, Avner BS, Su Y, van der Saag PT, Witte PL, Fiore S, Levine JS, Ucker DS (2006). Specific recognition of apoptotic cells reveals a ubiquitous and unconventional innate immunity. J Biol Chem 281, 20055–20067.

Cvetanovic M, Ucker DS (2004). Innate immune discrimination of apoptotic cells: repression of proinflammatory macrophage transcription is coupled directly to specific recognition. J Immunol 172, 880–889.

Devitt A, Moffatt OD, Raykundalia C, Capra JD, Simmons DL, Gregory CD (1998). Human CD14 mediates recognition of phagocytosis of apoptotic cells. Nature 392, 505–509.

Elliott MR *et al*. (2009). Nucleotides released by apoptotic cells act as a find-me signal to promote phagocytic clearance. Nature 461, 282–286.

Fadok VA, Bratton DL, Konowal A, Freed PW, Westcott JY, Henson PM (1998a). Macrophages that have ingested apoptotic cells in vitro inhibit proinflammatory cytokine production through autocrine/paracrine mechanisms involving TGF-β, PGE2, and PAF. J Clin Invest 101, 890–898.

Fadok VA, Warner ML, Bratton DL, Henson PM (1998b). CD36 is required for phagocytosis of apoptotic cells by human macrophages that use either a phosphatidylserine receptor or the vitronectin receptor ($\alpha_V\beta_3$). J Immunol 161, 6250–6257.

Gude DR, Alvarez SE, Paugh SW, Mitra P, Yu J, Griffiths R, Barbour SE, Milstien S, Spiegel S (2008). Apoptosis induces expression of sphingosine kinase 1 to release sphingosine-1-phosphate as a "come-and-get-me" signal. FASEB J 22, 2629–2638.

Guo X (2012). Surface plasmon resonance based biosensor technique: a review. J Biophotonics 5, 483–501.

Hanayama R, Tanaka M, Miwa K, Shinohara A, Iwamatsu A, Nagata S (2002). Identification of a factor that links apoptotic cells to phagocytes. Nature 417, 182–187.

Kim S, Elkon KB, Ma X (2004). Transcriptional suppression of interleukin-12 gene expression following phagocytosis of apoptotic cells. Immunity 21, 643–653.

Lidstone EA, Chaudhery V, Kohl A, Chan V, Wolf-Jensen T, Schook LB, Bashir R, Cunningham BT (2011). Label-free imaging of cell attachment with photonic crystal enhanced microscopy. Analyst 136, 3608–3615.

Meagher LC, Savill JS, Baker A, Fuller RW, Haslett C (1992). Phagocytosis of apoptotic neutrophils does not induce macrophage release of thromboxane B_2. J Leukoc Biol 52, 269–272.

Miyanishi M, Tada K, Koike M, Uchiyama Y, Kitamura T, Nagata S (2007). Identification of Tim4 as a phosphatidylserine receptor. Nature 450, 435–439.

Patel VA, Longacre A, Hsiao K, Fan H, Meng F, Mitchell JE, Rauch J, Ucker DS, Levine JS (2006). Apoptotic cells, at all stages of the death process, trigger characteristic signaling events that are divergent from and dominant over those triggered by necrotic cells: implications for the delayed clearance model of autoimmunity. J Biol Chem 281, 4663–4670.

Patel VA, Longacre-Antoni A, Cvetanovic M, Lee DJ, Feng L, Fan H, Rauch J, Ucker DS, Levine JS (2007). The affirmative response of the innate immune system to apoptotic cells. Autoimmunity 40, 274–280.

Reddy SM, Hsiao KH, Abernethy VE, Fan H, Longacre A, Lieberthal W, Rauch J, Koh JS, Levine JS (2002). Phagocytosis of apoptotic cells by macrophages induces novel signaling events leading to cytokine-independent survival and inhibition of proliferation: activation of Akt and inhibition of extracellular signal-regulated kinases 1 and 2. J Immunol 169, 702–713.

Ren Y, Xie Y, Jiang G, Fan J, Yeung J, Li W, Tam PK, Savill J (2008). Apoptotic cells protect mice against lipopolysaccharide-induced shock. J Immunol 180, 4978–4985.

Savill J, Dransfield I, Gregory C, Haslett C (2002). A blast from the past: clearance of apoptotic cells regulates immune responses. Nat Rev Immunol 2, 965–975.

Schlegel RA, Williamson P (2001). Phosphatidylserine, a death knell. Cell Death Differ 8, 551–563.

Scott RS, McMahon EJ, Pop SM, Reap EA, Caricchio R, Cohen PL, Earp HS, Matsushima GK (2001). Phagocytosis and clearance of apoptotic cells is mediated by MER. Nature 411, 207–211.

Shamah SM, Cunningham BT (2011). Label-free cell-based assays using photonic crystal optical biosensors. Analyst 136, 1090–1102.

Ucker DS, Jain MR, Pattabiraman G, Palasiewicz K, Birge RB, Li H (2012). Externalized glycolytic enzymes are novel, conserved, and early biomarkers of apoptosis. J Biol Chem 287, 10325–10343.

Voll RE, Herrmann M, Roth EA, Stach C, Kalden JR, Girkontaite I (1997). Immunosuppressive effects of apoptotic cells. Nature 390, 350–351.

Xiao YQ, Freire-de-Lima CG, Schiemann WP, Bratton DL, Vandivier RW, Henson PM (2008). Transcriptional and translational regulation of TGF-β production in response to apoptotic cells. J Immunol 181, 3575–3585.